

Modelling ocean circulation and ice – ocean interaction in the southeastern Weddell Sea

Malte Thoma¹, Klaus Grosfeld²,

Chris-Oliver Mohrholz¹, Manfred A. Lange¹

(1) Institute for Geophysics, University of Münster, Germany

(2) Department of Physics/MARUM, University of Bremen, Germany

Introduction

We describe the ocean general circulation model ROMBAX and its applications to the Eastern Weddell Ice Shelves (EWIS) in the Weddell Sea (Figure 1). We focus on the influence of Ice Shelf Water (ISW) production on the density stratification at present and under possible climate change scenarios. In addition, preliminary results of a coupled application of a dynamic ice-shelf model and the ocean model to the EWIS region are presented.

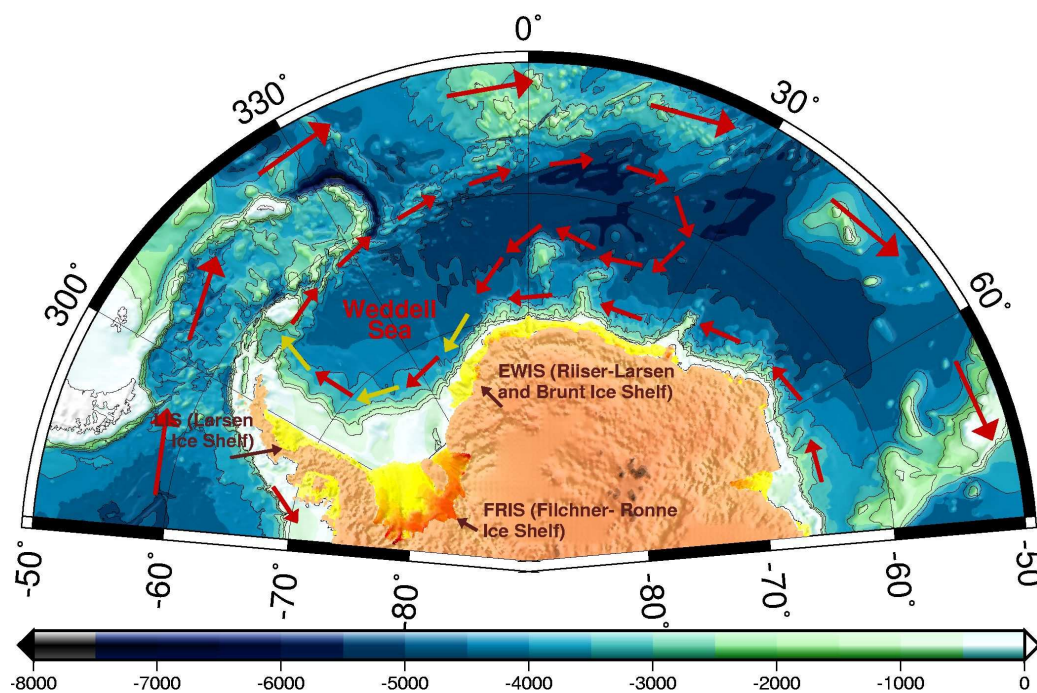


Figure 1: Major ocean currents in the Weddell Sea and the adjacent ocean basins. Long red arrows indicate the Antarctic Circumpolar Current, short red arrows the Weddell Gyre and to the south the Antarctic Coastal Current, and yellow arrows indicate the admixture of Ice Shelf Water. Ice shelves are marked in yellow to reddish colour, indicating increasing ice thicknesses towards the inland ice shown in copper (Data from Lythe *et al.*, 2001).

Ocean model and numerical code

The numerical ocean model ROMBAX (*Revised Ocean Model based on Bryan And Cox*) is based on a set of so-called primitive equations (e.g., Haidvogel & Beckmann, 1999; Griffies, 2004) which describe hydrodynamical flow on a sphere under the assumptions of the *Coriolis approximation* (vertical motion much smaller than horizontal motion) and the *thin-shell approximation* (fluid layer depth is small compared to the radius of the sphere). Additional approximations such as the *hydrostatic assumption*, the *Boussinesque approximation*, the *Rigid-lid approximation* and the assumption of *incompressibility* reduce the general flow equations, rendering them applicable for basin-scale to global ocean circulation modelling. The continuity equation ensures mass conservation, Laplace operators describe the diffusion of the conservative properties salinity and potential temperature, and the density is given by an empirical equation of state (Mellor, 1991). Several numerical schemes to describe the thermodynamic interaction between ocean and ice-shelf base are implemented, all based upon fundamental formulations ensuring heat and salt conservation (Holland & Jenkins, 1999) and an empirical function for the dependence of the freezing point temperature on ambient (Foldvik & Kvinge, 1974). In this study we use two different formulations for ice-ocean interaction: a simple bulk (two-equation) formulation and a probably more realistic (three-equation) formulation, considering the exchange coefficients, which are explicitly based on physical quantities.

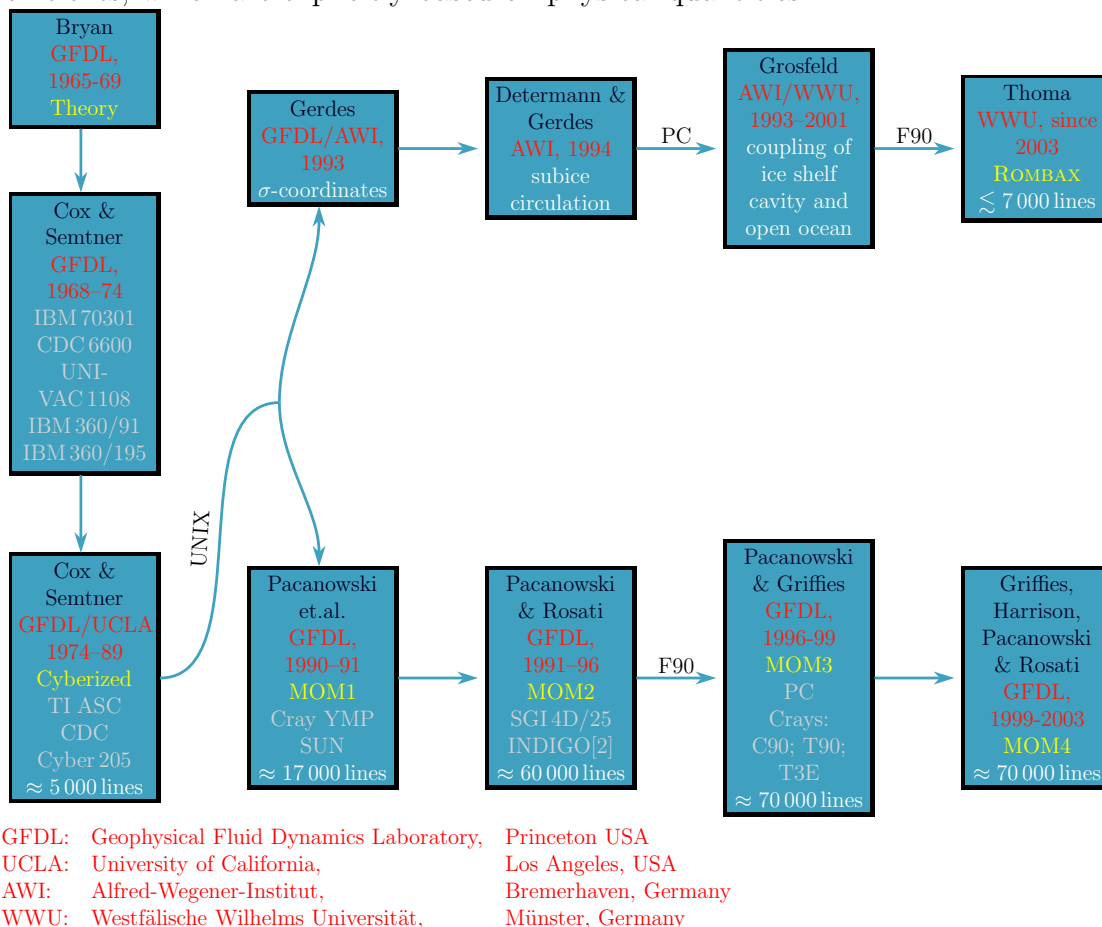


Figure 2: History and origin of ROMBAX.

The roots of the numerical code (Figure 2) trace back to the familiar Bryan (1969) and Cox (1984) model, which represents the base of the GFDL (Geophysical Fluid Dynamics Laboratory) Modular Ocean Model (MOM) developed in Princeton, USA. The GFDL has developed the model over the years to a worldwide accepted community model, improving the physics and implementing a number of different schemes and features, leading to the recently released MOM4 version (Griffies *et al.*, 2003). ROMBAX has been detached from the development of MOM by Gerdes (1993), who implemented σ -coordinates for a better representation of bedrock topography. Determann & Gerdes (1994) and Grosfeld *et al.* (1997) refined the model for its applicability to subice shelf circulation and combined open ocean – ice-shelf cavity circulation modelling, respectively. This high resolution numerical model has mainly been used in regional studies that describe the circulation in continental shelf regions of the Weddell Sea and Prydz Bay (e.g., Grosfeld *et al.*, 1997; Grosfeld & Gerdes, 1998; Grosfeld *et al.*, 1998; Gerdes *et al.*, 1999; Grosfeld *et al.*, 2001; Williams *et al.*, 2001; Nicolaus & Grosfeld, 2002).

The main drawback of this code (as for MOM3) was, however, the usage of the so called *slab* technique to propagate row-by-row through the model domain from south to north. Only three grid columns of the model domain are held in RAM memory at once while the rest is swapped to a (sometimes only virtual) disk. This technique was necessary at times during which computer memory was rare and expensive, but it needs more computational time due to frequent array copying. Furthermore, the additional code needed for the slab technique is very prone to errors as a result of code extensions. Based on these experiences, we have rewritten the code and implemented a number of features which results in more efficient debugging and additional developments. In addition, we have reimplemented the metric terms for advection and diffusion in the equation of momentum which have been omitted since Cox (1984).

Water mass formation in the vicinity of the EWIS

To investigate the ice-ocean interaction in the south-eastern Weddell Sea and the impact of freshwater fluxes onto the water-mass formation, geometric data records for bathymetry and ice draft are taken from the BEDMAP archive (Lythe *et al.*, 2001). Where bathymetry and ice draft contain inconsistencies, we adjusted the bedrock topography beneath the ice shelf in a way that forces a sub-ice shelf water column thickness of at least 30 m, by lowering the bedrock where necessary. The horizontal resolution of our model is 0.1° in south-north and 0.3° in west-east direction. In the vertical plane we apply ten σ -layers in the open ocean and beneath the ice shelf (each ranging from 2% to 23% of total water column thickness). In addition, we added four z-layers at the top of the open ocean, scaled to the draft of the ice-shelf edge which is assumed to be 100 m thick.

The ocean model is initialised with hydrographic data taken from Gouretski *et al.* (1999). Forcing at the ocean surface is achieved through climatological monthly winds after Kottmeier & Sellmann (1996), with freshwater fluxes according to ice-ocean interactions in the EWIS cavities. Furthermore temperatures and salinities at the ocean surface as well as at the northern and eastern model domain boundaries were obtained by applying a Newtonian damping scheme. A detailed discussion of the general flow pattern in

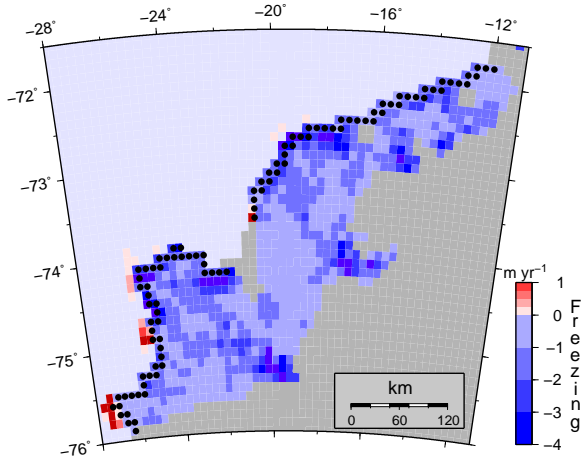


Figure 3: Melting (negative) and freezing (positive) in the EWIS region considering the explicit formulation for ice-ocean interaction.

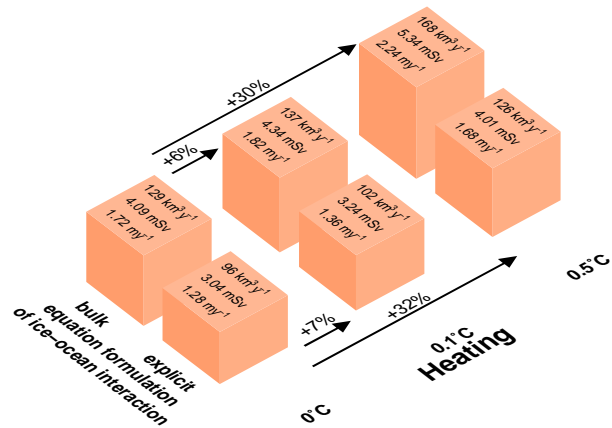


Figure 4: Net freshwater production from the EWIS for different parameterisations and assumed ocean warming in volume and Sverdrup. In addition, the mean melt rate of the EWIS region is given in m yr^{-1} .

the EWIS region is given by Thoma *et al.* (2004). Here we focus on the aspect of ISW production in the EWIS region and its impact on the water-mass formation in the coastal current of the eastern Weddell Sea.

In contrast to other ice shelves (e.g., the Filchner-Ronne or Ross Ice Shelves) where extended continental shelf areas prevent direct access of Warm Deep Water (WDW) to the ice-shelf cavities, the EWIS cavity is partly penetrated by the coastal current (Fahrbach *et al.*, 1994). By employing an explicit formulation for ice-ocean interaction, an average melt rate of 1.28 m yr^{-1} , corresponding to a volume of $96 \text{ km}^3 \text{ yr}^{-1}$, is calculated this is equivalent to a freshwater production of 3.04 mSv (Figure 3 and 4). Considering the simplified bulk formulation, significant higher (about 34%) melting rates are seen. A comparison of the estimated freshwater fluxes with previous field studies by Thomas (1973) and Fahrbach *et al.* (1994) reveals good agreement. This is probably a result of the small spatial resolution realised in our model compared to, e.g., model results from Timmermann *et al.* (2003) and Hellmer (2004). They use a much coarser grid, leading to an overestimated access of the coastal current into the ice-shelf cavity especially along narrow continental shelf regions (Nicolaus & Grosfeld, 2002). We suggest, that the velocity dependent explicit formulation of ice-ocean interaction reflects the dependency of basal melting on the flow regime much better, especially in this region where the small distance between ice-shelf cavity and coastal current leads to strong interactions between both systems.

To investigate the sensitivity of the EWIS region under changing climate boundary conditions, we perform studies for different warming scenarios based on observations (0.1°C , Fahrbach *et al.*, 2004) and Intergovernmental Panel on Climate Change (IPCC) (Leggett *et al.*, 1992) emission scenarios (0.5°C), respectively. The corresponding net melt rate for the moderate 0.1°C ocean warming scenario increases about 6%–7%, depending on the chosen parametrisation of ice-ocean interaction, compared to the control run (Figure 4). In the second more rigorous warming scenario for the Weddell Sea, we estimate a strong melt rate increase of 30% (or 32%, respectively).

Figure 5a shows a meridional transect of the density stratification in the southern Weddell Sea at 27° W, from 76° S to 73° S for the control run. The glacial freshwater flux from the EWIS region leads to a density decrease in waters over the continental shelf, spreading out into the open ocean and influencing the density stratification. Based on results of a hypothetical model configuration, where the EWIS has been completely eliminated (Figure 5b) it is obvious that EWIS do not only affect the density on the continental shelf alone, it also influences the density stratification of the upper 500 m at least 100 km beyond the continental shelf in the open ocean. Hence, the spreading of isopycnals as consequence of glacial freshwater input leads to a stabilisation of the water column. In case of no ice-shelf coverage (Figure 5b), the continental shelf is flooded with dense waters formed during winter through sea ice formation and associated brine release. Overflow of these water masses induces subsequently an increased density in shallow and deep waters of the open ocean. This leads to a general destabilisation of the water column and causes deep convection in the open ocean. This process finally enhance vertical heat exchange and have a bearing on sea ice formation and the surface heat balance.

Ocean warming of 0.5°C strongly changes the density distribution (Figure 5c). Because of increased melting, the density over the continental shelf decreases significantly, compared to the present day situation (Figure 5a). The freshwater export, in addition to the induced warming of the water column leads to a density decrease of the upper water column and a subsidence of higher-density waters (e.g., 1027.8 kg m⁻³ contour line). Hence, stabilisation of the water column occurs, preventing the occurrence of deep convection and bottom water formation.

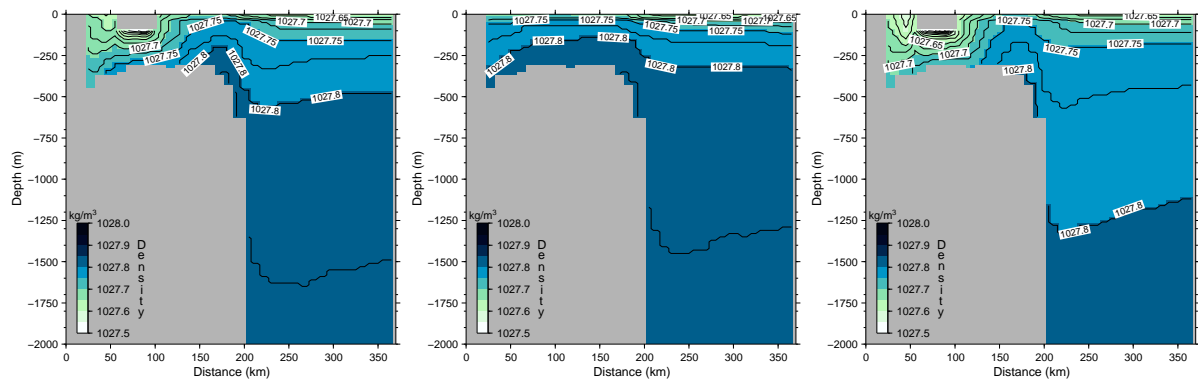


Figure 5: Density profile across a track at the southern tip of EWIS, (a) with and (b) without ice-shelf coverage. (c) shows the density distribution for a sensitivity experiment, by assuming an ocean warming of 0.5°C. The density is calculated for temperatures and salinities at surface pressure.

Preliminary results of a coupled shelf ice – ocean model for the southeastern Weddell Sea

Up to now, only static ice-shelf configurations have been investigated with respect to ocean interactions. However, basal melting or freezing influences the ice shelf draft and,

hence, the ice dynamics. To investigate the dynamic response of the ice-shelves in the EWIS region to present day and possibly future changed oceanic boundary conditions, we started to simulate a coupled ice-shelf – ocean system with both, ice shelf and ocean as dynamic model components.

Coupling between a numerical ice-shelf model and an ocean general circulation model has originally been described by Grosfeld & Sandhäger (2004) for an idealised geometry. Figure 6 sketches the input and output parameters of the present numerical models and indicates the exchange parameters. Since coordinate systems and resolutions of CISIP (Coupled Ice-Shelf – Ice-sheet comPUtation) (Cartesian, 2.5 km) and ROMBAX (spherical, $0.3^\circ \times 0.1^\circ$) are different, interpolation and coordinate transformation is done through the coupling module CiROM.

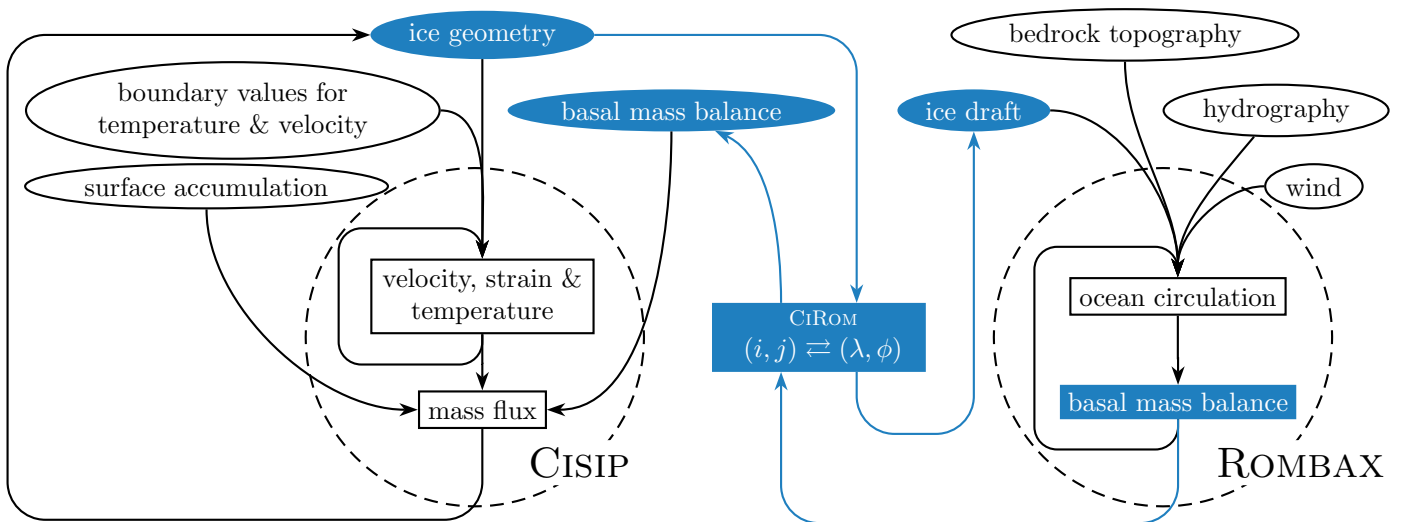


Figure 6: Coupling of ice model CISIP and ocean model ROMBAX via the module CiROM. Loops in dashed circles indicate iterations until a convergence criterion is fulfilled. The exchange values between the models and the coordinate transformation are indicated in coloured nodes.

The numerical ice-shelf model CISIP is based on commonly used balance equations for momentum, mass and heat. Combined with Glen's flow law, the incompressibility constraint and the ice-shelf approximation, which implies a depth-independent flow regime, a set of nonlinear differential equations are obtained, according to MacAyeal & Thomas (1986). In the numerical code, developed by Sandhäger (2000), the vertical coordinate is represented by σ -coordinates (Mayer, 1996). An overview of the ice-shelf model and some special approximations are given in Grosfeld & Sandhäger (2004).

Since the BEDMAP data (Lythe *et al.*, 2001) are insufficient to represent EWIS at high resolution (2.5 km), the ice-shelf geometry has been refined by data gathered from Liu *et al.* (2001) and BAS *et al.* (2002) (Figure 7). The simulated velocity field is presented in Figure 8. While flow directions of our model result correspond well with observations from satellite images (e.g., Figure 7, left) and field studies (e.g., Thomas, 1973), the absolute velocity near the ice-shelf front is about 20% smaller than observed.

As the ice-shelf flow of several ice-shelf regions is influenced by fractures and crevasses,

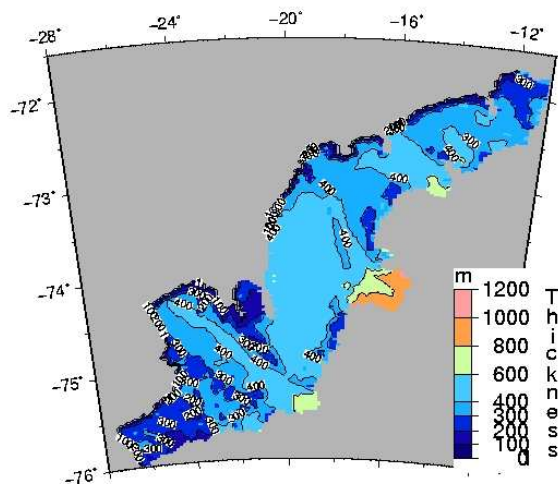
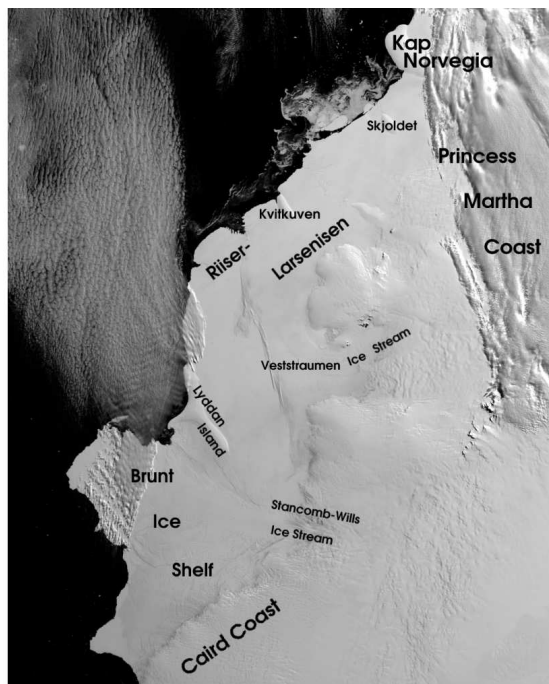


Figure 7: Satellite image (from February 19th 2003 by Scambos *et al.*, 2001 (updated current year)); morphological features are indicated (left) and the initial ice thickness after Lythe *et al.* (2001), Liu *et al.* (2001) and BAS *et al.* (2002) (right) for the EWIS.

Sandhäger (2003) introduced a simple numerical scheme to handle these structures, leading to a decoupling of grid cells and, hence, to higher flow velocities. Currently we attempt to improve this scheme in order to apply it to the EWIS region, where large areas are dominated by inhomogeneous structures and a very complex flow pattern.

Despite these limitations, first results of a coupled simulation for the EWIS region are obtained. Figure 9 compares the calculated basal melt rate from CISIP, derived from the continuity equation of mass conservation and an estimated surface accumulation rate, with the basal melt rate derived by the ocean model. To be consistent with the ice-shelf geometry used in CISIP, the ice draft for ROMBAX is generated from the ice-shelf model results. After the first coupling cycles of the ice-shelf and ocean models, the calculated basal mass balance of both model components does obviously not coincide. The basal mass balance, derived from the ice-shelf model, depicts regions with extended basal freezing, especially in multi-fractured regions like the Stancomb-Wills

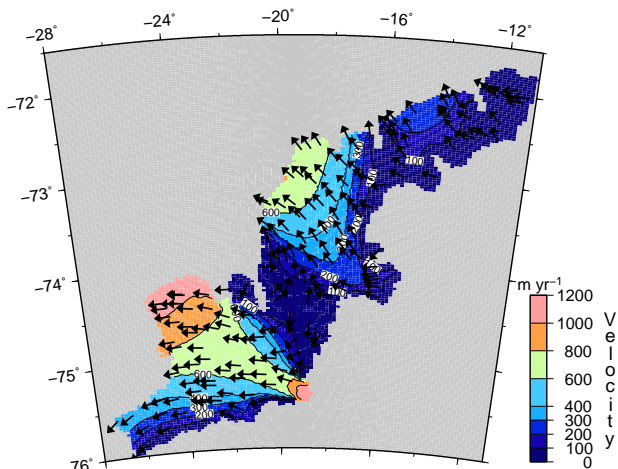


Figure 8: Absolute values of the horizontal flow velocity, arrows indicate flow direction.

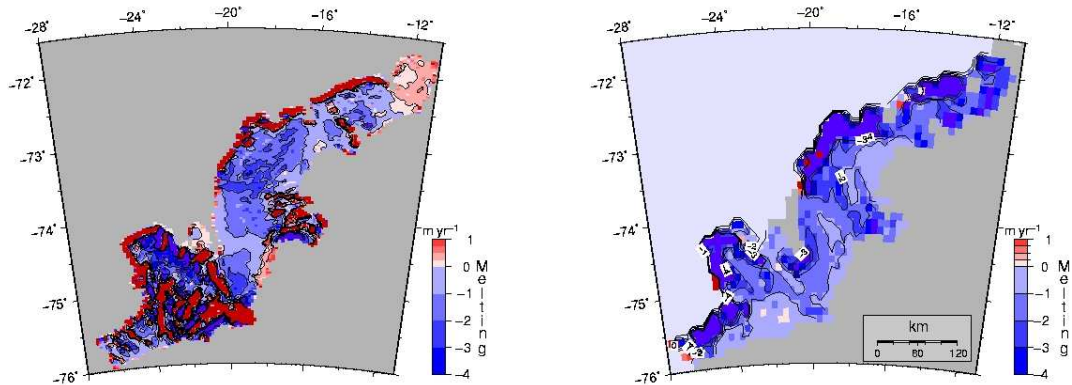


Figure 9: Basal melt rate calculated with the ice-shelf model C1SIP (left) and the ocean model ROMBAX (right).

Stream. Due to the lack of explicit fracture zone consideration in the ice-shelf model, the velocities of the outlet glaciers are too small, resulting in a tailback of ice which drains from the inland into the ice shelf. In the model, this process is compensated by basal freezing, the only free component in the mass balance equation. In regions with less fracture zones like the central part of Riiser-Larsenisen, both models produce consistent melting of about -2 m yr^{-1} . Basal freezing along the ice-shelf front in the ice-shelf model results from the fixed ice-shelf geometry, preventing the ice shelf from spreading onto the open ocean.

Outlook

Our modelling efforts show that the EWIS is an important region for water-mass conditioning and formation in the Weddell Sea. Due to the narrow continental shelf, the ice shelf and consequently the glacial freshwater flux is highly sensitive and vulnerable to changed water-mass conditions of the coastal current. The investigation of the coupled ice-shelf – ocean system represents a key-task to understand present and the future evolution of the coupled ice-shelf – ocean system in the southern Weddell Sea sector and its feedback to the regional climate development. Therefore, our next modelling steps are intended to

- implement fractures into the ice-shelf model to improve the simulated ice dynamics,
- apply the high resolution model to the southern Weddell Sea sector, and
- analyse the influence of changed climatic boundary conditions on the ocean circulation and ISW production in the southern Weddell Sea.

Acknowledgements: This work is part of the German CLIVAR/marin-project. Funding by the Bundesministerium für Bildung, Wissenschaft, Forschung und Technologie (bmb+f) der Bundesrepublik Deutschland, contract 03F0377C, is gratefully acknowledged.

References

- BAS, SPRI & WCMC. 2002. Antarctic Digital Database, Version 4.0, , Scientific Committee on Antarctic Research, Cambridge, U.K.
- BRYAN, K. 1969. A numerical method for the study of the circulation of the world ocean, *Journal of Computational Physics*, 4, 347–376.
- COX, M. D. 1984. A primitive equation, 3-dimensional model of the ocean, *GFDL Ocean Group Technical Report No. 1*, Princeton University.
- DETERMANN, J. & GERDES, R. 1994. Melting and freezing beneath ice shelves: Implications from a 3-d ocean circulation model, *Annals of Glaciology*, 20, 413–419.
- FAHRBACH, E., ROHARDT, G., SCHRÖDER & STRASS, V. 1994. Transport and structure of the Weddell Sea, *Annales Geophysicæ*, 12, 840–855.
- FAHRBACH, E., HOPPEMA, M., ROHARDT, G., SCHRÖDER, M. & WISOTZKI, A. 2004. Decadal-scale variations of water mass properties in the deep Weddell Sea, *Ocean Dynamics*, 54, 77–91.
- FOLDVIK, A. & KVINDE, T. 1974. Conditional instability of sea water at the freezing point, *Deep-Sea Research*, 21, 169–197.
- GERDES, R. 1993. A primitive equation ocean circulation model using a general vertical transformation. Part 1: Description and testing of the model, *Journal of Geophysical Research*, 98, 14,683–14,701.
- GERDES, R., DETERMANN, J. & GROSFELD, K. 1999. Ocean circulation beneath filchner-ronne ice shelf from three-dimensional model results, *Journal of Geophysical Research*, C7, 15,827–15,841.
- GOURETSKI, V., JANCKE, K., REID, J., SWIFT, J., RHINES, P., SCHLITZER, R. & YASHAYAEV, I. 1999. WOCE Hydrographic Programme Special Analysis Centre, Atlas of Ocean Sections, CD-ROM.
- GRIFFIES, S. M., 2004. *Fundamentals of ocean climate models*, Princeton University Press, Princeton.
- GRIFFIES, S. M., HARRISON, R. C., M. J. PACANOWSKI & ROSATI, A., 2003. *A Technical Guide to MOM4*, NOAA/Geophysical Fluid Dynamics Laboratory, Princeton.
- GROSFELD, K. & GERDES, R. 1998. Circulation beneath the Filchner Ice Shelf and its sensitivity to changes in the oceanic environment: a case study, *Annals of Glaciology*, 27, 99–104.
- GROSFELD, K. & SANDHÄGER, H. 2004. The evolution of a coupled ice shelf – ocean system under different climate states, *Global Planetary Change*, 42, 107–132, doi:10.1016/j.gloplacha.2003.11.04.
- GROSFELD, K., GERDES, R. & DETERMANN, J. 1997. Thermohaline circulation and interaction beneath ice shelf cavities and the adjacent open ocean, *Journal of Geophysical Research*, 102, 15,595–15,610.
- GROSFELD, K., HELLMER, H. H., JONAS, M., SANDHÄGER, H., SCHULTE, M. & VAUGHAN, D. G. 1998. Marine ice beneath filchner ice shelf: Evidence from a multi-disciplinary approach, *Antarctic Research Series*, 75, 319–339.
- GROSFELD, K., SCHRÖDER, M., FAHRBACH, E., GERDES, R. & MACKENSEN, A. 2001. How iceberg calving and grounding change the circulation and hydrography in the Filchner Ice Shelf - ocean system, *Journal of Geophysical Research*, 106, 9039–9055.
- HAIDVOGEL, D. B. & BECKMANN, A., 1999. *Numerical ocean circulation modeling*, Imperial College Press, London.
- HELLMER, H. H. 2004. Impact of Antarctic ice shelf basal melting on sea ice and deep ocean properties, *Geophysical Research Letters*, 31, 1–4, L10307, doi:10.1029/2004GL019506.
- HOLLAND, D. M. & JENKINS, A. 1999. Modeling thermodynamic ice-ocean interaction at the base of an ice shelf, *Journal of Physical Oceanography*, 29, 1787–1800.
- KOTTMEIER, C. & SELLMANN, L. 1996. Atmospheric and oceanic forcing of Weddell Sea ice motion, *Journal of Geophysical Research*, 101, 20,809–20,824.
- LEGGETT, J., PEPPER, W. J. & SWART, R. J. 1992. Emissions scenarios for ipcc: An update, in *The Supplementary Report to the IPCC Scientific Assessment*, edited by J. T. Houghton, B. A. Callander, & S. K. Varney, pp. 69–95, Cambridge University Press.
- LIU, H., JEZEK, K., LI, B. & ZHAO, Z. 2001. Radarsat antarctic mapping project digital elevation model version 2, Boulder, CO: National Snow and Ice Data Center. Digital media, digital media, Internet Page: <http://nsidc.org/data/nsidc-0082.html>.
- LYTHE, M. B., VAUGHAN, D. G. & THE BEDMAP CONSORTIUM. 2001. BEDMAP: A new ice thickness and subglacial topographic model of the Antarctic, *Journal of Geophysical Research*, 106, 11,335–11,351.
- MACAYEAL, D. & THOMAS, R. 1986. The effects of basal melting on the present flow of the Ross Ice Shelf, Antarctica, *Annals of Glaciology*, 32, 72–86.
- MAYER, C. 1996. Numerische Modellierung der Übergangszone zwischen Eisschild und Schelfeis, *Scientific*

Reports 214, Ber. zur Polarforschung.

- MELLOR, G. L. 1991. An equation of state for numerical models of oceans and estuaries, *Journal of Atmospheric and Oceanic Technology*, 8, 609–611.
- NICOLAUS, M. & GROSFELD, K. 2002. Ice – ocean interaction underneath the Antarctic ice shelf Ekströmisen, *Polarforschung*, 72, 17–29.
- SANDHÄGER, H. 2000. Quantifizierung eisdynamischer und massenhaushaltsrelevanter Basisgren eines antarktischen Inland-Schelfeis-Systems unter Einsatz eines numerischen Fliemodells, Ph.D. thesis, Westfälische Wilhelms-Universität Münster.
- SANDHÄGER, H. 2003. Numerical study on the influence of fractures and zone of weakness on the flow regime of Larsen Ice Shelf, *FRISP*, 14.
- SCAMBOS, T., RAUP, B., J., B. & COMPILERS. 2001 (updated current year). Images of Antarctic ice shelves, digital media.
- THOMA, M., GROSFELD, K. & LANGE, M. A. 2004. The role of Eastern Weddell Ice Shelves for water mass formation in the southern Weddell Sea, *Antarctic Science*, submitted.
- THOMAS, R. H. 1973. The dynamics of the Brunt Ice Shelf, Coats Land, Antarctica, *Scient. Rep. 79*, British Antarctic Survey.
- TIMMERMANN, R., BECKMANN, A. & HELLMER, H. H. 2003. The role of sea ice in the fresh water budget of the Weddell Sea, *Annals of Glaciology*, 33, 419–424.
- WILLIAMS, M. J. M., GROSFELD, K., WARNER, R. C., GERDES, R. & DETERMANN, J. 2001. Ocean circulation and ice - ocean interaction beneath the Amery Ice Shelf, Antarctica, *Journal of Geophysical Research*, 106, 22,383–22,400.